BBA - Molecular Basis of Disease 1869 (2023) 166764

Contents lists available at ScienceDirect

BBA - Molecular Basis of Disease

journal homepage: www.elsevier.com/locate/bbadis

Depletion of Mcpip1 in murine myeloid cells results in intestinal dysbiosis followed by allergic inflammation

Weronika Szukala [a,b,1], Magdalena Pilarczyk-Zurek [c,1], Justyna Folkert [c], Jerzy Kotlinowski [a], Joanna Koziel [c,*,2], Jolanta Jura [a,*,2]

[a] Jagiellonian University, Faculty of Biochemistry, Biophysics and Biotechnology, Department of General Biochemistry, Gronostajowa 7, 30-387 Krakow, Poland
[b] Jagiellonian University, Doctoral School of Exact and Natural Sciences, Lojasiewicza 11, 30-348 Krakow, Poland
[c] Jagiellonian University, Faculty of Biochemistry, Biophysics and Biotechnology, Department of Microbiology, Gronostajowa 7, 30-387 Krakow, Poland

ARTICLE INFO

Keywords:
MCPIP1
Skin contact allergy
Gut-skin axis
Intestinal dysbiosis
C/EBP
IL-4

ABSTRACT

MCPIP1 (called also Regnase-1) is a negative regulator of inflammation. Knockout of the *Zc3h12a* gene, encoding Mcpip1 in cells of myeloid origin (Mcpip1^{MKO}), has a pathological effect on many organs. The aim of this study was to comprehensively analyze pathological changes in the skin caused by Mcpip1 deficiency in phagocytes with an emphasis on its molecular mechanism associated with microbiome dysbiosis.

Mcpip1^{MKO} mice exhibited spontaneous wound formation on the skin. On a molecular level, the Th2-type immune response was predominantly characterized by an increase in *Il5* and *Il13* transcript levels, as well as eosinophil and mast cell infiltration. Irritation by DNFB led to a more severe skin contact allergy in Mcpip1^{MKO} mice. Allergic reactions on the skin were strongly influenced by gut dysbiosis and enhanced systemic dissemination of bacteria. This process was followed by activation of the C/EBP pathway in peripheral macrophages, leading to local changes in the cytokine microenvironment that promoted the Th2 response. A reduced bacterial load inhibited allergic inflammation, indicating the role of intestinal dysbiosis in the development of skin diseases. Our results clearly show that MCPIP1 in phagocytes is an essential negative regulator that controls the gut-skin axis.

1. Introduction

Skin diseases are becoming an increasingly serious problem worldwide, and both external and internal factors, such as exposure to UV radiation, frequent use of cosmetics containing irritating chemicals, diet, pharmaceuticals and/or chronic stress, can significantly influence the incidence of these diseases [1–3]. Modern lifestyles and changes toward sterility in sanitary conditions lead to the imbalance of immune homeostasis. Consequently, changes in microbiota abundance and profile of organs such as the skin and intestines have been observed. This phenomenon, called dysbiosis, contributes to the etiology of many diseases. There is a growing body of data showing the interdependence between the gut microbiota profile and skin disorders [4]. This applies, inter alia, to the correlation between the composition and diversity of the gut microbiota and allergic diseases, including eczema [5–8]. We and others have recently shown that a CCCH-zinc finger protein, called MCPIP1 (or Regnase-1), acting as an RNase, is important for regulating skin homeostasis [9–11]. MCPIP1 is a negative regulator of immune and inflammatory responses and controls the half-life of transcripts encoding key mediators of both processes [12,13]. When examining a mouse model in which the *Zc3h12a* gene encoding Mcpip1 in keratinocytes (Mcpip1^{EKO} model) had been knocked out, we observed the appearance of wounds on the skin of aging mice. Moreover, the balance between proliferation markers, differentiation markers and inflammatory regulators associated with the skin of these mice was disturbed. As a consequence, strong local inflammation in Mcpip1^{EKO} mice induced systemic inflammation indicated by enlarged lymph nodes and splenomegaly [14].

A more complex phenotype is found in mice in which *Zc3h12a* is deleted in cells of myeloid origin, particularly macrophages and

Abbreviations: DTH, delayed type hypersensitivity; IMQ, imiquimod; GI, Gastrointestinal tract; CFU, colony forming unit; Th2, T helper type 2.

* Corresponding authors at: Faculty of Biochemistry, Biophysics and Biotechnology, Jagiellonian University, ul. Gronostajowa 7, 30-387 Kraków, Poland.
E-mail addresses: joanna.koziel@uj.edu.pl (J. Koziel), jolata.jura@uj.edu.pl (J. Jura).
[1] These first authors contributed equally
[2] These corresponding authors contributed equally

https://doi.org/10.1016/j.bbadis.2023.166764
Received 21 March 2023; Received in revised form 17 May 2023; Accepted 23 May 2023
Available online 29 May 2023

granulocytes (LysM^{Cre}Mcpip1$^{loxP/loxP}$ mice, here Mcpip1^{MKO}). The general characterization of this model has already been described [15,16]. Elderly Mcpip1^{MKO} mice develop spontaneous inflammatory syndromes, including cachexia, splenomegaly, lymphadenopathy and multiorgan inflammation.

Here, we used Mcpip1^{MKO} mice to demonstrate the strong relationship between the condition of the skin and the amount and diversity of the gut microbiota under conditions of immunologically hyperresponsive myeloid cells.

2. Material and methods

2.1. Mice

To obtain mice with myeloid-specific knockout of the *Zc3h12a* gene encoding Mcpip1, the Cre-loxP system was used as described previously [15]. The animals were cohoused under specific pathogen-free (SPF) conditions in accordance with the Guide for the Care and Use of Laboratory Animals (Directive 2010/63/EU of the European Parliament). The mice used in this study were sex- and age-matched littermates. The animal experiments were carried out under a license from the 2nd Local Institutional Animal Care and Use Committee in Krakow (nr 72/2021).

2.2. DTH response

Cutaneous contact with the chemical irritant 2,4-dinitrofluorobenzene (DNFB) was used to induce a delayed type hypersensitivity (DTH) response, according to the Röse et al. protocol [17]. Briefly, 12- and 24-week-old control and Mcpip1^{MKO} mice were epicutaneously sensitized on shaved abdomens with 25 μl of 0.5 % DNFB (Sigma-Aldrich) diluted in acetone-corn oil (4:1, v/v) (Sigma-Aldrich) on day −5. On day 0, all the mice were challenged on one ear with 15 μl of 0.3 % DNFB. Then, after 24 h, the mice were sacrificed, and the ears were collected. The subsequent increase in ear thickness was measured 24 h later with a digital micrometer (Mitutoyo, Kawasaki, Japan).

2.3. Imiquimod-induced skin inflammation

The Imiquimod (IMQ) mouse model of psoriasis-like skin inflammation was used as previously described by van der Fits [18]. We applied a daily topical dose of 62.5 mg of commercially available IMQ cream (5 %) (Aldara; 3 M Pharmaceuticals) on the shaved backs of 6- to 8-week-old control and Mcpip1^{MKO} mice for 4 days. Vehicle cream (Vaseline) was used as a control of experiment. The clinical PASI (Psoriasis Area and Severity Index) score was used to indicate the severity of inflammation by scoring: redness, scaling and thickness on a scale from 0 to 4 (none, slight, moderate, marked and very marked). Skin thickness was measured daily with a digital micrometer.

2.4. Antibiotic treatment

For antibiotic treatment, 10-week-old, cohoused control and Mcpip1^{MKO} mice were given broad-spectrum antibiotic agents, including ampicillin (Sigma-Aldrich) (1 g/l), neomycin (Sigma-Aldrich) (1 g/l), vancomycin (Sigma-Aldrich) (0.5 g/l), ciprofloxacin (Sigma-Aldrich) (0.2 g/l), erythromycin (Sigma-Aldrich) (0.02 g/l) and metronidazole (Sigma-Aldrich) (0.5 g/l), dissolved in drinking water for 6 weeks.

2.5. Sample collection

After sacrificing the mice, the whole GI tracts were segmented into the ileum, cecum and colon. The cecum was resected and weighed, and its contents were collected for microbiological analysis. The length and diameter of the colon were measured. The ileum and colon fragments were subsequently opened, and the contents from each segment were thoroughly harvested by collection and subjected to microbiological analysis. Lungs were snap-frozen in liquid nitrogen and stored at −80 °C until RNA/DNA isolation. Spleens, livers, lymph nodes and skin were homogenized in 1 ml PBS and subjected to microbiological analysis. PBS-washed colonic tissue, feces, skin and ear tissue specimens were snap-frozen in liquid nitrogen and stored at −80 °C until RNA/DNA isolation.

2.6. RNA isolation and quantitative real-time PCR

Total RNA isolation, reverse transcription and real-time PCR were performed as described previously [14]. The sequences of the primers (Sigma-Aldrich) are listed in Supplementary Table S1.

2.7. Histological staining

Skin, ear, lymph node and distal colon tissue specimens were fixed in 4 % formaldehyde overnight, processed for dehydration and embedded in paraffin for further histological staining. Otherwise, for immunofluorescence staining, skin specimens were incubated in 30 % sucrose and then embedded in Tissue-Tek O.C.T. (Fisher Scientific). Furthermore, 5–8 μm sections were cut and stained with H&E (Sigma-Aldrich) using a standard protocol. To investigate mast cell and eosinophil infiltration, sections were stained with 0.01 % toluidine blue (Sigma-Aldrich) and with eosinophil and mast cell staining kits (Abcam, Cambridge, UK) according to the manufacturer's protocol. For Alcian blue staining, the colon tissue was fixed in Carnoy's fixative solution (dry methanol: chloroform: glacial acetic acid in the ratio of 6:3:1) before embedding. Slides were stained with an Alcian blue solution (1 % Alcian blue, pH 2.5, Sigma-Aldrich) for 30 min and counterstained by the routine H&E method. For immunofluorescence staining of skin sections, the procedure was performed as described previously [14]. Sections were examined using Leica Application Suite X (LAS X) image acquisition software and a Leica DMC5400 fluorescence microscope (Leica Microsystems). All figures were prepared using ImageJ and CorelDraw. Antibodies against the following were used for staining: Hoechst 33258 (Sigma-Aldrich), rat CD206 (1:200; eBioscience), rabbit CD68 (1:200; Abcam), goat Alexa Fluor 488 anti-rabbit (1:600; Invitrogen), and goat Alexa Fluor 594 anti-rat (1:600; Invitrogen).

2.8. FISH

Fragments of colon, lymph nodes, spleens and livers were embedded in paraffin and cut to a thickness of 5 μm using a microtome. Paraffin sections were rehydrated after two washes with PBS. The slides were covered with a solution of lysozyme at 10 mg/ml in PBS for 20 min at 37 °C and washed twice with PBS. After 30 min of incubation in hybridization buffer (20 mM Tris·HCl pH 7,4, 0.9 M NaCl, 0.1 % SDS), the slides were incubated for 4 h at 56 °C in hybridization buffer containing 20 nM fluorescent probes. After washing twice, the slides were covered for 10 min with DAPI (0.125 g/ml in PBS), washed in PBS and mounted in DAKO. The 16S rRNA-targeted oligonucleotide probe used was Eub338 5′-FITC-GCTGCCTCCCGTAGGAGT-3′. The slides were examined with a fluorescence microscope.

2.9. Bacterial analysis

All homogenized samples were plated at a volume of 100 μl in required dilutions on selective media: MacConkey agar plates (Sigma-Aldrich) for gram-negative bacteria, bile esculin agar for *Enterococcus* (BHL), MRS for *Lactobacillus* (Sigma-Aldrich), and Columbia agar and Scheadler broth (Sigma-Aldrich) as nonselective media for aerobes and anaerobes, respectively. Plates were incubated for 1–2 days at 37 °C under optimal conditions. All CFUs were counted.

2.10. NGS sequencing analysis of the microbiota

Genomic DNA was isolated from fecal pellets using the QIAamp DNA Stool kit (QIAGEN) according to the manufacturer's instructions. The concentration of genomic DNA was measured prior to the library preparation procedure by fluorimetry using PicoGreen reagent (Life Technologies). The measurement was taken on a Tecan Infinite microplate reader. Specific sequences were used to amplify the selected region and prepare the library primers 341F and 785R. PCR was performed using Q5 Hot Start High-Fidelity 2× Master Mix (New England Biolabs) under the reaction conditions recommended by the manufacturer. Sequencing was carried out on a MiSeq sequencer using paired-end technology (2 × 300 nt) and the MiSeq Reagent Kit v3 (600-cycle) (Illumina) according to the manufacturer's protocol. The reads obtained in NGS were analyzed using QIIME software and the base of sequence reference SILVA_v_138. The number of reads matching to each genome was counted. The relative abundance of bacterial Phylum, Genous, and Families was calculated according to NGS read numbers and was expressed as the percentage [19,20].

2.11. ELISA

Skin tissue specimens that had been frozen and stored at −80 °C were homogenized in PBS containing 1 % Triton X-100 (Bio-Shop) and protease inhibitor (Roche). The total amount of protein in each sample was assessed using a bicinchoninic acid assay. The levels of the Il-4 and Il-5 cytokines were measured in duplicate using a mouse DuoSet ELISA (R&D Systems) according to the manufacturer's protocol.

2.12. Blood analysis

The analysis of blood morphology was performed using the Scil Animal Care Company ABC Hematology Analyzer. The concentration of inflammatory mediators in plasma was performed as described previously by Dobosz et al., using BD Cytometric Bead Array [16].

2.13. Isolation of monocytes from bone marrow

Bone marrow cells were isolated from femurs and tibias of mice using previously described methods [21]. Briefly, marrow was extracted by centrifuging (10'000 ×*g*, 40 s) bones in 1.5 ml tubes and resuspended in RPMI 1640 supplemented with 10 % FBS and 1 % penicillin/streptomycin. The retained erythrocytes were lysed in 0.155 M NH_4Cl, cells were washed two times in RPMI 1640 supplemented with 10 % FBS and 1 % penicillin/streptomycin and centrifuged (300 ×*g*, 5 min, 4 °C). 2 mln/tube bone marrow cells were seeded into sterile plastic wells (Corning) for further experiments at 37 °C with 5 % CO_2. Adherent cells, constituting a population of monocytes, were stimulated with LPS (10 ng/ml), CpG (0.3 uM), *E. coli* or *Lactobacillus* (isolated from mice feces at a MOI 1:50). RNA isolation was performed.

2.14. Statistical analysis

Statistical analyses, including one-way ANOVA and Student's *t*-test, were performed using GraphPad Prism 8 (GraphPad Software). All experiments were performed in at least 3 independent biological replicates (with at least 4 mice per each experiment).

3. Results

3.1. *Mcpip1*^{MKO} mice exhibit a dominant Th2-type immune response in the skin

To study the role of the MCPIP1 protein in the crosstalk between keratinocytes and immune cells, we used Mcpip1^{MKO} mice, in which Mcpip1 is specifically deleted in cells of myeloid origin. Next, we performed a thorough biochemical and microbiological multiorgan characterization of Mcpip1^{MKO} and control (Mcpip1$^{loxP/loxP}$) mice at two developmental stages: 12 weeks old (young) and 24 weeks old (adult). Although 12-week-old Mcpip1^{MKO} mice did not exhibit any obvious inflammatory skin phenotype, within the next 2 months, mice started to scratch themselves, and most of the 24-week-old mice developed lesions located on the ears, neck and down to the middle of the back (Fig. 1A). General blood morphology analysis of adult Mcpip1^{MKO} mice revealed that eosinophilia (Fig. 1B) correlated with an increase in the concentration of total immunoglobulin E (IgE) classes (Fig. 1C), which is characteristic of an allergic reaction.

To investigate the molecular background of the observed skin pathologies in adult Mcpip1^{MKO} mice, we carried out qRT–PCR to determine the expression profiles of the most typical inflammatory factors in the skin. We noticed activation of both Th1- (T helper type 1) and Th2-type immune responses; however, the Th2-dependent response was more pronounced. In particular, we found that only the mRNA level of *Ifng* (*interferon gamma*), a major cytokine produced by Th1 cells, increased in the skin of young (12-week-old) and adult (24-week-old) Mcpip1^{MKO} mice compared to control mice (Fig. 1D). The mRNA levels of other proinflammatory cytokines, such as *Tnfa, Il6, Il1a/b, Il36a/g, Il33* and the *S100a9* antibacterial peptide, were similar in the healthy skin of young and adult Mcpip1^{MKO} mice compared to control mice at the same age. However, the mRNA levels of *Tnfa, Il6, Il1b, Il33* and *S100a9* increased profoundly within the lesional skin of adult Mcpip1^{MKO} mice. On the other hand, we noticed strong activation of several Th2-type cytokines in both healthy and lesional skin of adult Mcpip1^{MKO} mice. Notably, the expression of *Il5* and *Il13* mRNAs in the skin increased 16- and 5-fold in adult and 3.5- and 2.6-fold in young Mcpip1^{MKO} mice compared to control mice at the same age, respectively. The mRNA level of *Il4*, also secreted by Th2 cells, was elevated in the skin of adult Mcpip1^{MKO} mice; however, the increase was statistically significant only in lesional skin. This increase in transcriptional expression was also noticed at the protein level, particularly for Il-4 and Il-5, within both healthy and lesional skin of adult Mcpip1^{MKO} mice compared to control mice (Fig. 1E). In addition, the transcript level of *Ccr3* (*C—C chemokine receptor type 3*), coding for the receptor on Th2 cells, eosinophils and basophils, was consistently 3.5-fold elevated within the healthy skin of adult Mcpip1^{MKO} mice compared to control mice (Fig. 1D). In turn, the transcript level of *Cxcr3* (*C-X-C motif chemokine receptor 3*), encoding the receptor expressed mostly on Th1 cells, was unchanged. We also found that the mRNA levels of Th17-type cytokines such as *Il17* and *Il23a* were unchanged. Interestingly, in the healthy and lesional skin of adult Mcpip1^{MKO} mice, we noticed an increase in the expression of transcripts encoding the cytokine Il-10 (1.5-fold and 3.2-fold, respectively). This anti-inflammatory cytokine produced by regulatory T cells (Tregs) may serve as a mechanism for counteracting the proinflammatory reactions observed in the lesional skin of adult Mcpip1^{MKO} mice. However, the mRNA levels of *Il12a* and *Tgfb2* (*transforming growth factor beta 2*) were unaltered.

The activation of the inflammatory response in Mcpip1^{MKO} mouse skin was also indicated by increased transcript levels of genes encoding chemokines such as Ccl2/Mcp-1, Ccl5/Rantes, Ccl7/Mcp-3, Ccl11/Eotaxin, and Ccl20/Mip-3α (3.5-, 6.5-, 2.3-, 3.5- and 2.4-fold in the healthy skin of adult Mcpip1^{MKO} mice compared to control mice, respectively) (Fig. 2A). These chemokines promote the infiltration of mast cells and eosinophils, as was also observed in the dermis of Mcpip1^{MKO} mice (Fig. 2B-D). There was no infiltration of these granulocytes in the skin of control mice. Next, immunostaining analysis revealed the infiltration of M2 macrophages (CD68/CD206 double positive) in the skin of Mcpip1^{MKO} mice (Fig. 2E). This observation was correlated with a tendency to upregulate the transcript level of *Ym1* (statistically significant for lesional skin), a marker of alternatively activated macrophages (Fig. 2F). Thus, the characterization of Mcpip1^{MKO} mouse skin revealed the pathological changes typical of allergic inflammation.

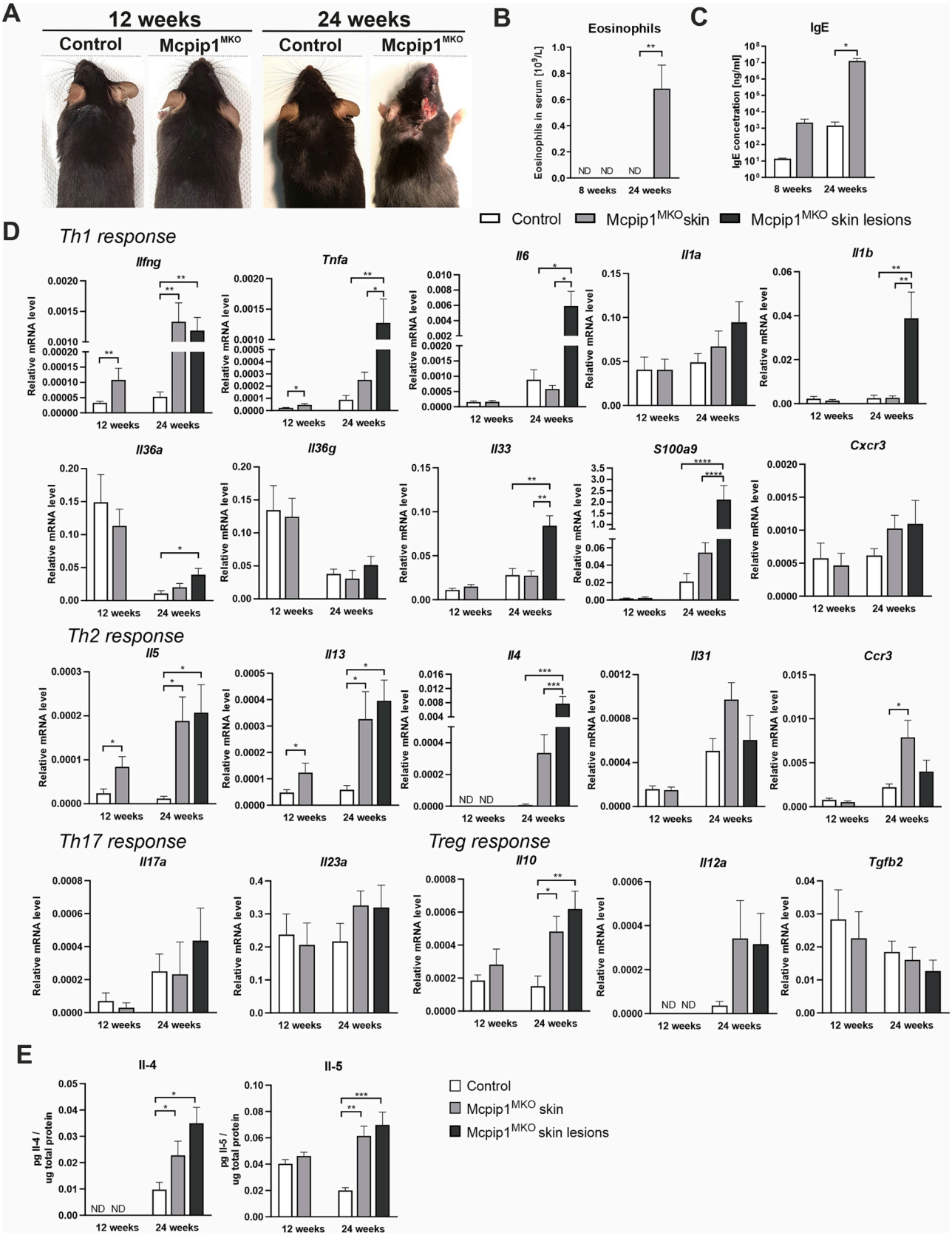

Fig. 1. Mice with myeloid-specific knockout of Mcpip1 develop Th2-type skin inflammation. A. Representative photographs of 12- and 24-week-old control and Mcpip1^{MKO} mice. B. Concentration of eosinophils in the blood of 8- and 24-week-old mice ($n = 3$). C. Concentration of total IgE classes in plasma ($n = 5–9$). D. qRT–PCR analysis of *Ifng, Tnfa, Il6, Il1a/b, Il36a/g, Il33, S100a9, Cxcr3, Il5, Il13, Il4, Il31, Ccr3, Il17a, Il23a, Il10, Il12a* and *Tgfb2* expression levels ($n = 7–9$). *Ef2* was used as a reference control. E. Protein levels of Il-4 and Il-5 obtained by ELISA ($n = 5$). Data are shown as the mean ± SEM. *P values*: $^*P < 0.05$, $^{**}P < 0.01$, $^{***}P < 0.001$. ND – not detected by qRT–PCR (a value of zero was given for statistics). Scale bar: 100 μm.

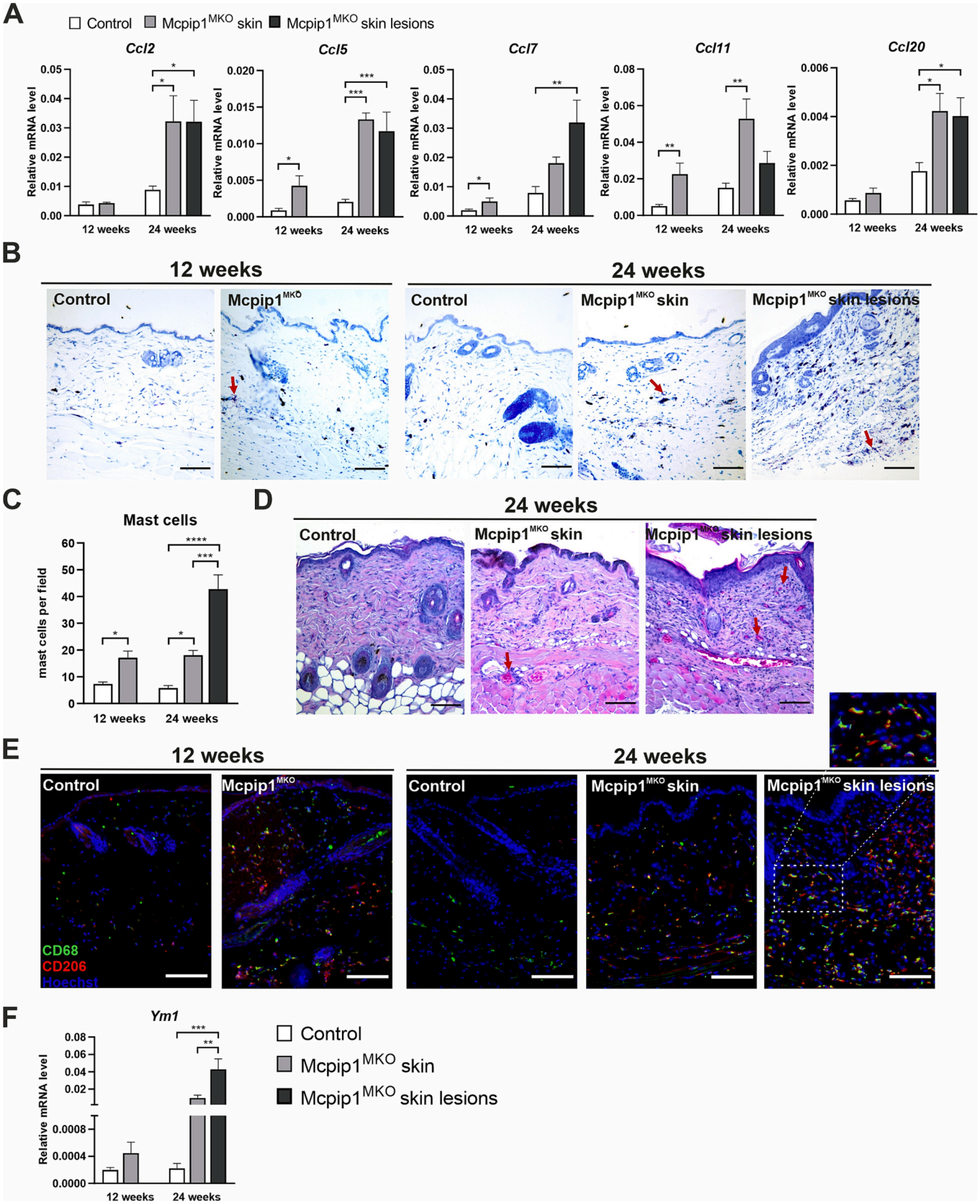

Fig. 2. Mcpip1^{MKO} mouse skin infiltrated by granulocytes. A. qRT–PCR analysis of *Ccl2, Ccl5, Ccl7, Ccl11* and *Ccl20* expression levels ($n = 7–9$). *Ef2* was used as a reference control. B. Toluidine blue staining of the skin of 12- and 24-week-old control and Mcpip1^{MKO} mice. Arrows indicate mast cells. C. The average number of mast cells counted per field in five independent fields per section ($n = 5$). D. Eosinophil staining of the skin of 24-week-old mice. Arrows indicate eosinophils. E. Immunofluorescence staining of CD68 and CD206 in skin sections. F. qRT–PCR analysis of *Ym1* expression levels. Data are shown as the mean ± SEM. *P values*: $^{*}P < 0.05$, $^{**}P < 0.01$, $^{***}P < 0.001$. Scale bar: 100 μm.

3.2. Loss of myeloid Mcpip1 intensified the delayed-type hypersensitivity response

To determine whether the loss of myeloid Mcpip1 function in mice could induce skin contact allergy, we induced a delayed-type hypersensitivity (DTH) response with the chemical irritant DNFB. Mice were sensitized on the shaved abdomen with 0.5 % DNFB, and 5 days later, local allergy inflammation was induced by challenging the ear with 0.3 % DNFB (Fig. 3A). Both 12- and 24-week-old Mcpip1^{MKO} mice showed an intensified DTH response, as demonstrated by a significant increase in ear swelling compared to that in control mice (Fig. 3B-C). This enhanced response was further characterized by increased *Cxcl1, Cxcl2, Ccl5, Ccl11, Il4, Il5,* and *Il6* transcript levels (Fig. 3D). Furthermore, histological and toluidine blue staining revealed increased granulocyte infiltration (Fig. 3E-F). These results clearly demonstrate the increased sensitivity to skin contact allergy in Mcpip1^{MKO} mice.

Next, we utilized a classic model of psoriasis-like skin inflammation induced by imiquimod (IMQ). We applied cream containing IMQ daily for 4 consecutive days to the shaved backs of 6- to 8-week-old control and Mcpip^{MKO} mice. Then, skin thickness and the Psoriasis Area and Severity Index (PASI) score were measured daily (Suppl. Fig. 1A). We did not observe any significant acceleration or exacerbation in the development of psoriasis-like skin symptoms in Mcpip1^{MKO} mice (Suppl. Fig. 1B-D). Mcpip1^{MKO} mice showed a slight increase in redness after topical treatment with the control cream (Vaseline) compared to control mice, again indicating greater skin sensitivity. Moreover, on day 4 of treatment, at the histological level, we noticed an increase in epidermal thickness (Suppl. Fig. 1E-F). However, the cumulative PASI scores of the Mcpip1^{MKO} and control mice were unaltered (Suppl. Fig. 1C).

3.3. Myeloid Mcpip1 deficiency leads to dysbiosis in gut microbial communities

The development of allergic diseases is highly regulated by the host microbiome [22]. Therefore, our objective was to estimate the influence of Mcpip1 deficiency in phagocytes on its composition in the GI tract. Microbiological analysis of mouse feces showed a significant increase in total bacterial numbers in samples collected from the colons and ceca of 24-week-old Mcpip1^{MKO} mice compared to their littermate controls (Fig. 4A). Notably, we did not observe differences in the ileum (Fig. 4A). Analysis of 12-week-old mice confirmed the above observation, indicating that the increase in the total bacterial numbers precedes the

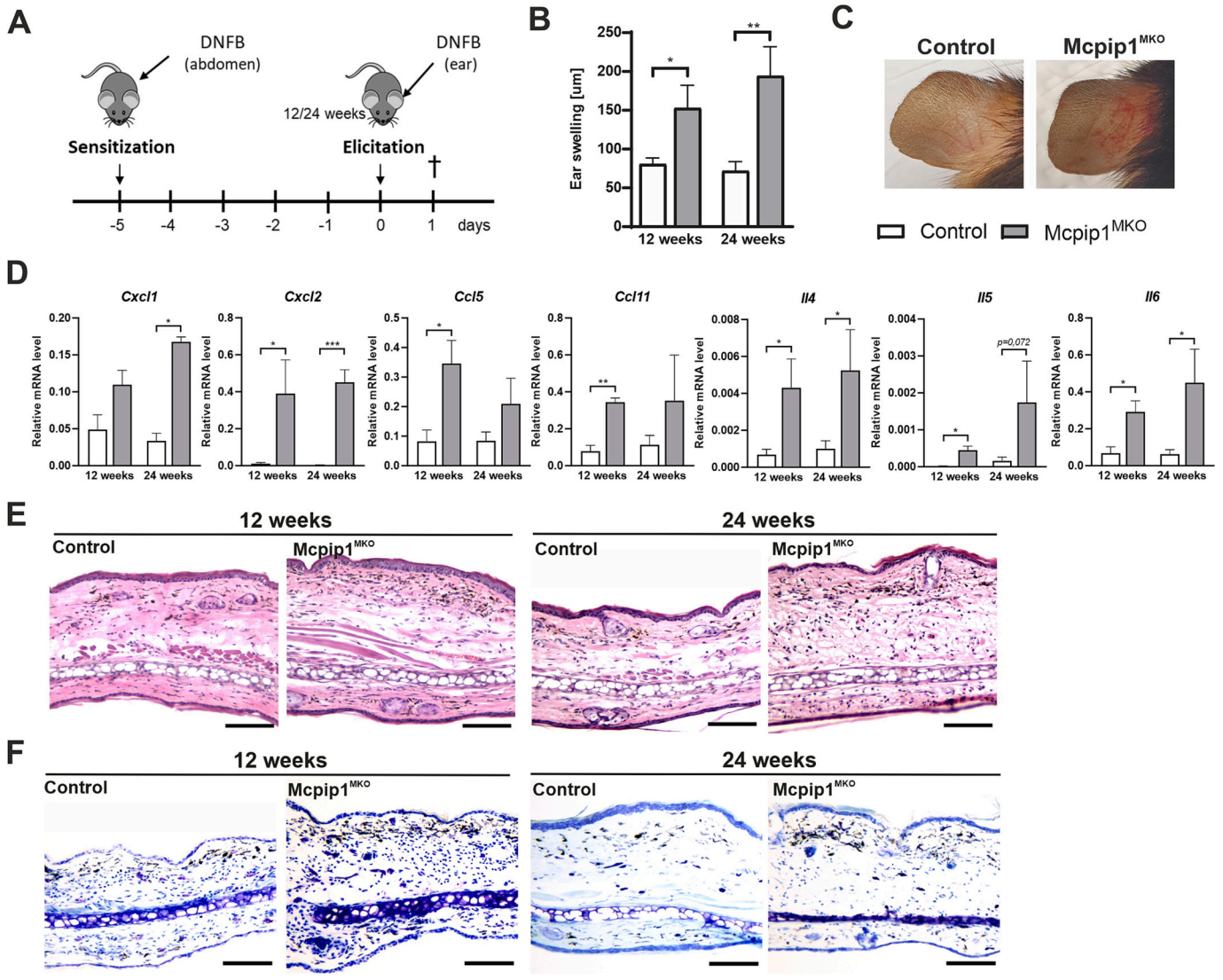

Fig. 3. Increased delayed-type hypersensitivity observed in Mcpip1^{MKO} mice. A. Schematic diagram of the DTH response to the DNFB experimental protocol. B. Ear swelling measured 24 h after DNFB challenge ($n = 4–7$). C. Representative photographs of ears after DNFB challenge. D. qRT–PCR analysis of *Cxcl1, Cxcl2, Ccl5, Ccl11, Il4, Il5* and *Il6* expression levels ($n = 4–7$). Data are shown as the mean ± SEM. *P values:* $^*P < 0.05$, $^{**}P < 0.01$. E. Representative H&E staining of 12- and 24-week-old control and Mcpip1^{MKO} ear sections after DNFB challenge. F. Toluidine blue staining. Scale bar: 100 μm.

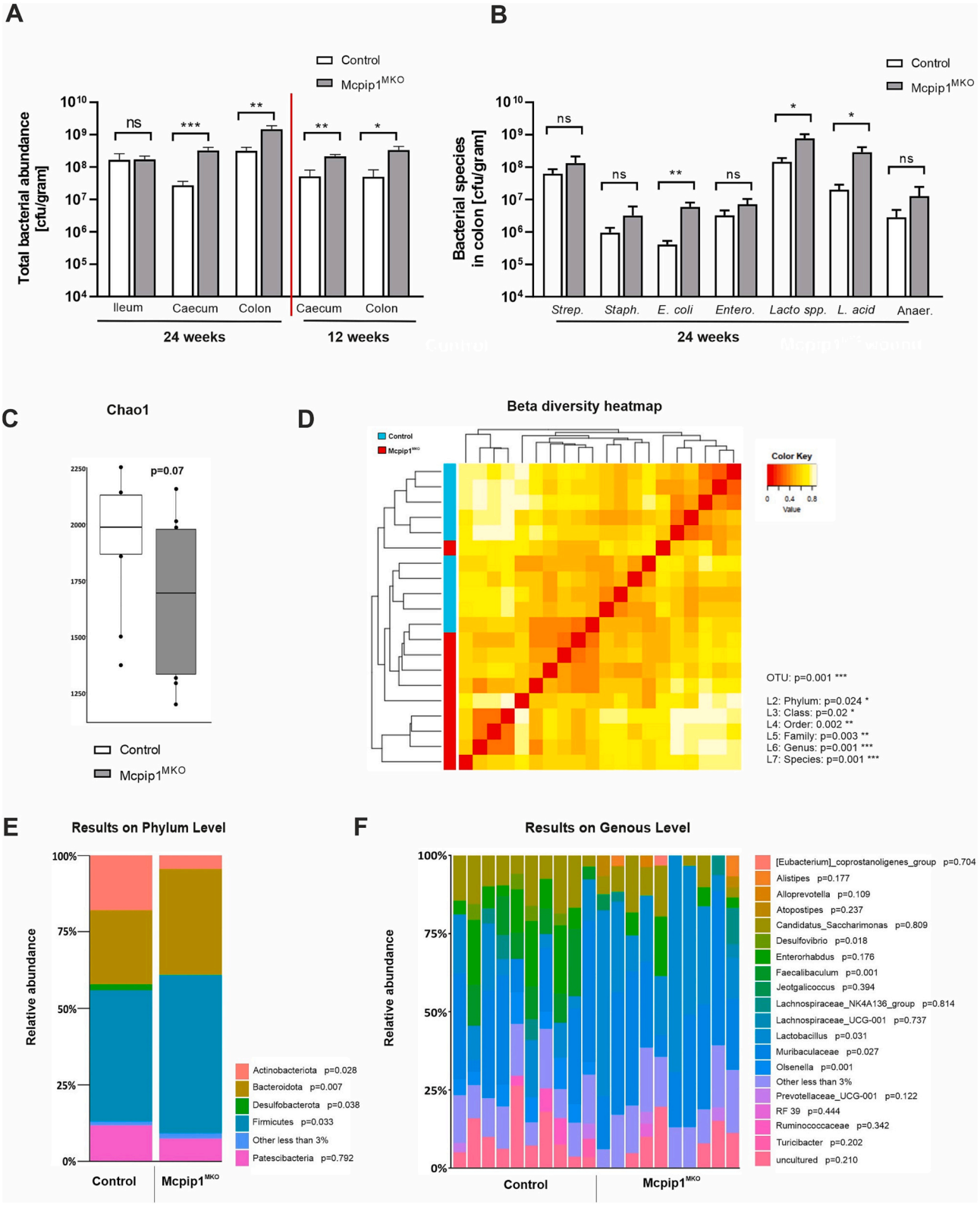

Fig. 4. Gastrointestinal dysbiosis caused by Mcpip1 deficiency. A. Comparison of the total number of bacteria in particular sections of the GI tract in 24- and 12-week-old mice ($n = 44$). Data are shown as the mean ± SEM. *P value:* $^{*}P < 0.05$, $^{**}P < 0.01$, $^{***}P < 0.001$, ns = nonsignificant. B. Qualitative microbiological analysis of colon feces obtained on the basis of the classic microbiological culture method in 24-week-old mice ($n = 34$). NGS analysis of fecal samples isolated from 24-week-old control and Mcpip1^{MKO} mice ($n = 20$). C. Chao's index of species richness in the alpha diversity parameter was pretested for compliance with the normal distribution using the Shapiro–Wilk test. D. Representative beta diversity analysis of operational taxonomic units (OTUs) ($P = 0.001$) and examined bacterial taxa with statistical evidence. Beta-diversity statistical analysis was performed using the PERMANOVA test. E. The relative abundance of bacterial phyla and genera in control and Mcpip1^{MKO} mice was calculated according to NGS read numbers and is expressed as a percentage. The difference in the share of individual taxa between the control and Mcpip1^{MKO} mice was analyzed using the ALDEx2 package and the Kruskal–Wallis test.

appearance of skin lesions (Fig. 4A). Therefore, using the classic microbial identification method, we investigated changes in species composition in the cecum and colon. Analysis of 24-week-old mice showed a significant increase in *Lactobacillus* spp. and *Escherichia coli* populations in the cecum and colons of Mcpip1^{MKO} mice compared to control mice (Fig. 4B, Suppl. Fig. 2A). In addition, an increase in the population of *Lactobacillus acidophilus* was observed in the colon (Fig. 4B). To confirm that Mcpip1 deficiency triggers gastrointestinal dysbiosis, a metataxonomic next-generation sequencing (NGS) analysis was performed. There were no statistically significant differences in the number of species according to Chao's index of species richness (Fig. 4C), while beta diversity analysis showed significant dysbiosis in Mcpip1^{MKO} mice compared to control mice (Fig. 4D). The distribution of bacterial phyla revealed the presence of expected components in the gut microbiome of mice, while we observed a significant increase in the abundance of *Firmicutes* (number of reads (n.r.): control 0.428 versus Mcpip1^{MKO} 0.517; $p = 0.033$) and *Bacteroidetes* (n.r.: control 0.242 vs. Mcpip1^{MKO} 0.346; $p = 0.007$) in Mcpip1^{MKO} mice (Fig. 4E). Consequently, the family *Lactobacillaceae* (belonging to *Firmicutes*) was dominant in Mcpip1^{MKO} mice (n.r.: control 0.107 vs. Mcpip1^{MKO} 0.306, $p = 0.021$) (Suppl. Fig. 2E), which was confirmed at the genetic level (Fig. 4F). Additionally, we examined the changes in the skin microbiota and found no difference in the incidence but a slight increase in the total number of bacteria in Mcpip1^{MKO} mice (Suppl. Fig. 2F-G). Taken together, these data indicate that Mcpip1 deficiency in myeloid cells causes intestinal dysbiosis.

3.4. Systemic dissemination of the gut microbiome is controlled by myeloid Mcpip1

Changes in the intestinal bacterial composition can lead to increased translocation of bacteria to lymphoid organs, thus shaping the inflammatory response in distal organs, including the skin [23]. Therefore, we analyzed intestinal permeability to bacteria by examining the translocation of microorganisms to the spleen and liver. We found a significant increase in bacterial incidence and load in Mcpip1^{MKO} mice (Fig. 5A-D). The lymph nodes were enlarged only in Mcpip1^{MKO} mice, and microbiological analysis revealed a high total bacterial number that reached 10^3–10^4 CFU (Fig. 5E). The enhanced bacterial dissemination was confirmed with fluorescence in situ hybridization (FISH) analysis (Fig. 5F). Detailed examination of the species showed a preferential distribution of *E. coli* and *Lactobacillus* spp. but not L. *acidophilus* (Suppl. Fig. 2B-C) to the spleen and liver. *Lactobacillus* spp. and *L. acidophilus* were identified in all lymph nodes (100 %) isolated from Mcpip1^{MKO} mice, while the incidence of *E. coli* was approximately 40 % (Suppl. Fig. 2D). Collectively, these results show that changes in the composition of the gut microbiome are reflected in increased bacterial dissemination.

To identify the mechanism of enhanced translocation of the gut microbiome from the intestine, we performed a macroscopic examination of the gut. We found no significant changes in the colon length or diameter or in cecum weight (Fig. 5G-J). The architecture of the mucosa was also examined. Analysis of colon cross sections revealed no hyperplasia of epithelial cells, change in epithelial cell number of longitudinal crypts, and no visible ulceration, degeneration, or deformation of the crypt (Fig. 5L). Detailed histomorphological evaluation of colon sections revealed that there was no massive infiltration of inflammatory cells into the mucosal, submucosal or transmural area (Fig. 5L). Notably, we found a significant reduction in mucosal thickness in the cross section of the colon collected from Mcpip1^{MKO} mice compared to control mice (Fig. 5K, M). As a consequence of the reduced thickness of the mucous layer, we found a higher level of positive FISH staining in deep layers of the colon tissue (Fig. 5N). Therefore, Mcpip1 deficiency in myeloid cells promotes enhanced systemic dissemination of bacteria from the gut.

3.5. Increased DTH response is inhibited by antibiotic treatment

To evaluate whether differences in the gut microbiota contribute to the skin phenotype in Mcpip1^{MKO} mice, 10-week-old cohoused control and Mcpip1^{MKO} mice were given a mixture of antibiotics dissolved in water for 6 weeks, and the DTH response was measured using the same protocol as before (Fig. 6A). Antibiotic treatment limited the bacterial load and systemic dissemination (Suppl. Table 2). As expected, the general condition of Mcpip1^{MKO} mice was better, and an inflammatory response was not observed after antibiotic treatment. There was no increase in the level of inflammatory mediators (Il-6, Il-10, Mcp1, Ifn-γ, Tnf-α, IL-12p70) in the plasma of Mcpip1^{MKO} mice (Fig. 6B). Moreover, the majority of cytokine and chemokine transcript levels were similar in the skin of both control mice and Mcpip1^{MKO} mice after antibiotic treatment (Fig. 6C). However, the transcript levels of *Il5* and *Ccl5* were still elevated (3.7- and 3-fold change, respectively) in the skin of Mcpip1^{MKO} mice relative to control mice, although these increases were not as pronounced as in nontreated mice, as mentioned earlier (Fig. 1D, 2A).

The inflammatory response after DNFB challenge was also inhibited by antibiotic treatment. Notably, this was indicated by the lack of significant differences in ear swelling (Fig. 6D). At the histological level, we did not observe any enhanced infiltration of immune cells in the ear skin of control or Mcpip1^{MKO} mice (Fig. 6E-F). Furthermore, the cytokine transcript levels, evaluated by qRT–PCR, were unchanged between control and Mcpip1^{MKO} mice (Fig. 6G). Taken together, these observations confirm that reducing the overall gut microbiota and their systemic dissemination from the intestine is sufficient to inhibit the induction of a contact allergy and reduce the intensity of spontaneous skin inflammation.

3.6. Gut peripheral macrophages control the Th2 immune response via C/EBP regulation and IL-4 secretion

To identify the molecular mechanism of the Th2 response, we examined the expression of *Il4* mRNA in macrophages exposed to bacterial LPS, live bacteria isolated from Mcpip1-deficient mice and CpG motifs. We found significant upregulation of *Il4* mRNA (Fig. 7A) in macrophages from Mcpip1^{MKO} mice compared to those from control mice. Moreover, we found enhanced mRNA expression of *Cebpb* and *Cebpd* (Fig. 7B-C), transcription factors that are crucial regulators of IL-4 [24]. The obtained in vitro data corroborate intestinal tissue expression, as we found increased local levels of *Il4 and Cebpd* mRNAs in young mice and more intense upregulation in the colons of 24-week-old animals (Fig. 7D). Moreover, we observed increased levels of *Cebpd* mRNAs. The elevated level of *Gata3* (Fig. 7D) confirmed local activation of the Th2 response. Additionally, we found that other cytokines considered in certain Th2-associated disease models [25], including *Tslp, Il25* and *Il33*, remained unchanged (Fig. 7D). Collectively, the obtained data suggest that peripheral macrophages control the Th2 response through C/EBP regulation and IL-4 secretion. Therefore, we propose that myeloid MCPIP1 contributes significantly to the final identity of Th2 cells in the tissue environment.

4. Discussion

Microbial populations inhabiting the gastrointestinal system play a key role in human health by preventing the overgrowth of harmful pathogens, producing vitamins and metabolites, aiding in nutrient uptake and stimulating the immune system [26–28]. Microbial colonization starts at birth with exposure to the maternal microbiome and is then shaped by the host genetic background and exposure to the environment [29]. Functional and compositional alterations in the gut microbiota, called gut dysbiosis, appear in response to environmental or host-related changes and are associated with several chronic inflammatory disease states [30,31]. The inner surface of the gastrointestinal tract is covered

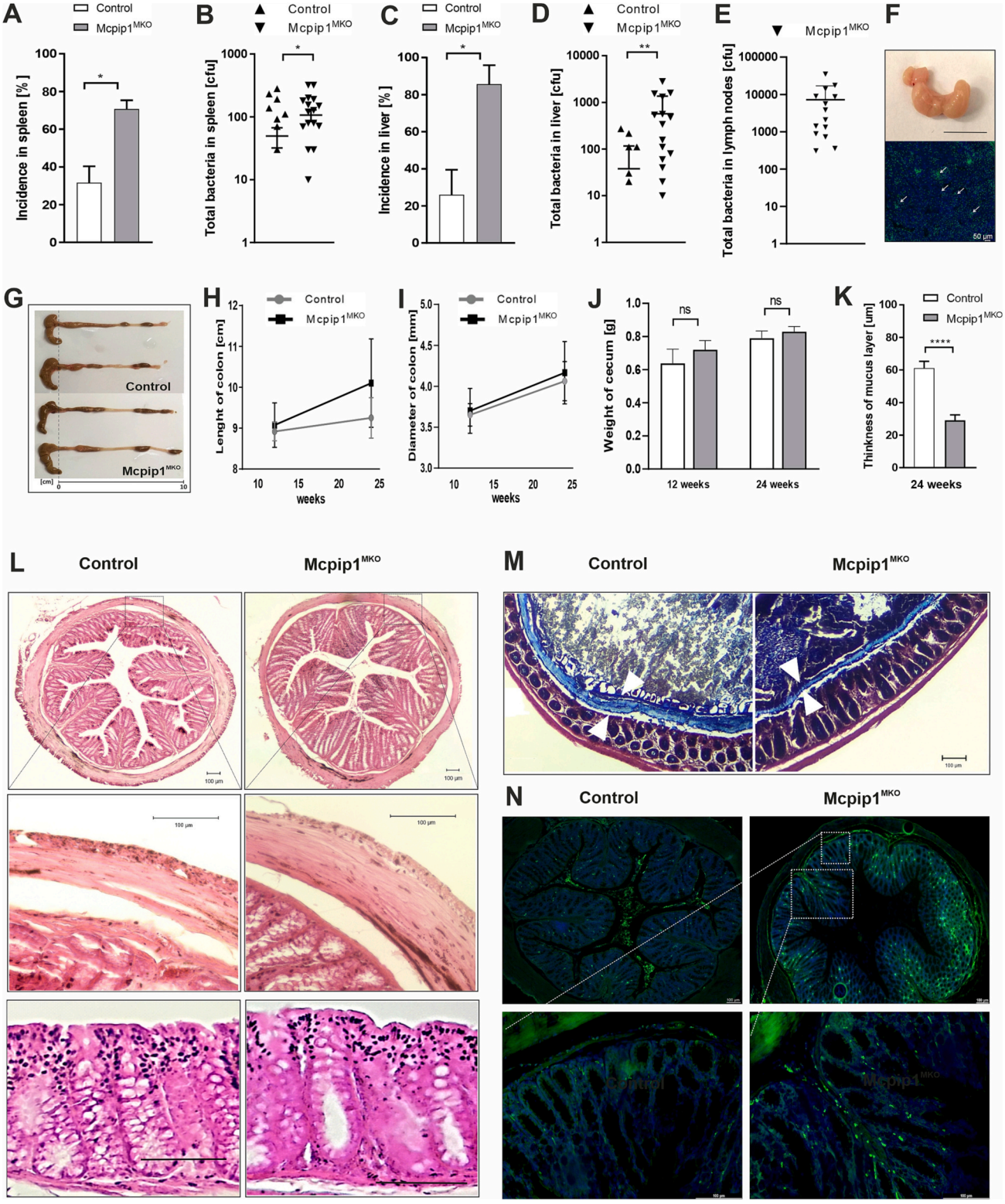

Fig. 5. Effect of Mcpip1 deficiency on the enhanced bacterial distribution and effectiveness of intestinal epithelial barrier function. A-D. Analysis of the incidence of bacteria and the total number of bacteria in the spleens ($n = 34$) and livers ($n = 34$) of control and Mcpip1^{MKO} mice. E. Total bacterial abundance in lymph nodes isolated from Mcpip1^{MKO} mice ($n = 15$). F. Representative photograph of a lymph node prepared from a Mcpip1^{MKO} mouse. FISH analysis of lymph nodes using the general bacterial probe EUB338-Alexa Fluor 488 (green) and DAPI nuclear staining (blue). Arrows indicate the fluorescent bacterial groups inside the lymph nodes. G. Representative image of a cecum and colon isolated from control and Mcpip1^{MKO} mice. H-J. Changes in the length (H) and diameter (I) of the colon and the weight of the cecum (J) prepared from control and Mcpip1^{MKO} mice ($n = 16$). L. Representative H&E staining of colon sections. K,M. Differences in the mucus layer (arrows) of the distal colon with fecal material obtained from 24-week-old control and Mcpip1^{MKO} mice assessed on Alcian blue and H&*E*-stained sections ($n = 16$). N. FISH analysis of colon cross sections. Arrows indicate the fluorescent bacterial groups found in the submucosa in Mcpip1^{MKO} mice, which were not observed in control mice. Data are shown as the mean ± SEM. *P value:* $^{*}P < 0.05$, $^{**}P < 0.01$, $^{***}P < 0.001$, ns = nonsignificant. Scale bars: 100 µm.

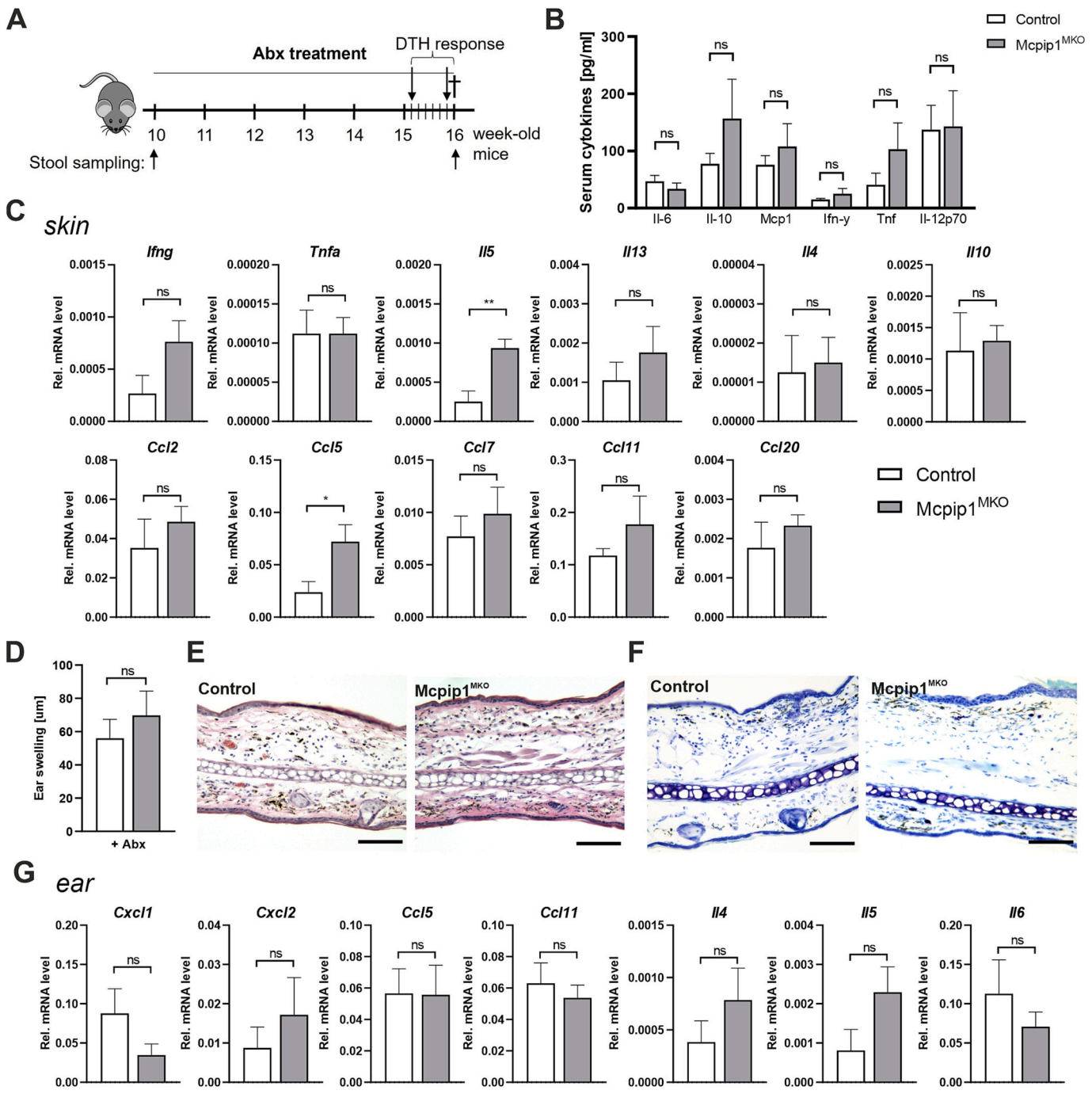

Fig. 6. The increased DTH response in Mcpip1^{MKO} mice is inhibited by antibiotic treatment. A. A schematic diagram of the sampling and antibiotic treatment of control and Mcpip1^{MKO} mice. B. Cytokine levels in the plasma of mice after antibiotic treatment ($n = 4–5$). C. qRT–PCR analysis of *Ifng, Tnfa, Il5, Il13, Il4, Il10, Ccl2, Ccl5, Ccl7, Ccl11* and *Ccl20* expression levels ($n = 4–5$). D. Ear swelling measured 24 h after DNFB challenge ($n = 4–5$). E. Representative H&E staining. F. Toluidine blue staining of ear sections after DNFB challenge. G. qRT–PCR analysis of *Cxcl1, Cxcl2, Ccl5, Ccl11, Il4, Il5* and *Il6* expression levels ($n = 4–5$). Data are shown as the mean ± SEM. *P values:* $^{*}P < 0.05$, $^{**}P < 0.01$. Scale bar: 100 μm. ns – nonsignificant.

by epithelial cells. Under physiological conditions, the harmful effect of the microbiota on the activation of immune cells in the gut and inflammatory response is minimized by a separation of the intestinal epithelium from the microbiota by a mucus layer. This layer is formed by mucin glycoproteins secreted by specialized epithelial cells called goblet cells and is a component of the innate immune system [32]. The thickness and integrity of the mucin layer protect against undesirable activation of the epithelium and penetration of bacteria through the intestinal walls.

Here, we described the consequences of changes in the gut microbiome on skin conditions using a mouse model in which the gene encoding Mcpip1 is knocked out in myeloid cells. The microbiome profile of Mcpip1^{MKO} mice showed a reduction in alpha diversity ($p = 0.07$) and a significant difference in beta diversity at all taxonomic levels, including the phylum level ($p = 0.024$), which is a characteristic marker observed in patients with atopic diseases and allergies [33–35]. The observed increase in the intestinal microbiota does not promote an inflammatory reaction in the gut. Histological analysis of the intestine in Mcpip1-deficient mice revealed no defects and no differences in pathomorphological alterations. The only aberration was a significant

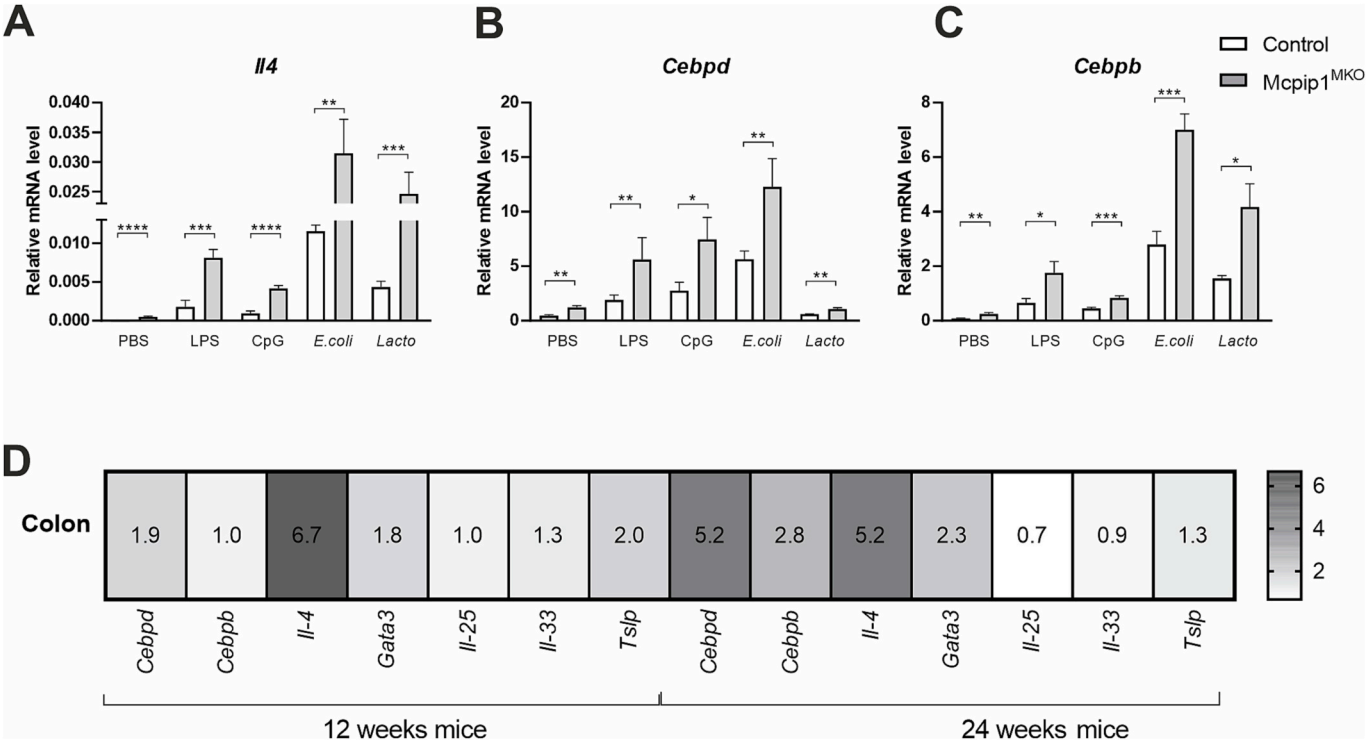

Fig. 7. The effect of Mcpip1 deficiency on macrophage response and the regulation of gene expression related to Th2 activation. A-C The expression of *Il4, Cebpd,* and *Cebpb* by BM cells stimulated for 6 h with LPS, CpG, *E. coli* and *Lactobacillus* (MOI 1:50) ($n = 12$). D Heatmap representing the changes in the expression of genes in the colons of Mcpip1^{MKO} mice. Relative mRNA levels were determined by qRT–PCR. Gene expression in wild-type animals was established as 1.

impairment of the mucus layer. It is likely that the reduction in the mucosal layer of Mcpip1^{MKO} mice resulted in systemic diffusion of the gut microbiome, demonstrated by an increased number of intestinal bacteria in peripheral organs. We propose that this phenomenon led to the increased skin sensitivity of Mcpip1^{MKO} mice. The significant role of Mcpip1 in the balance of skin homeostasis has already been described; however, studies have mainly focused on its expression in keratinocytes [9–11,14]. Here, we demonstrated that intestinal dysbiosis triggered by the lack of Mcpip1 in myeloid cells also resulted in deleterious consequences for the skin. Notably, we found significant evidence for the development of allergic inflammation in the skin of Mcpip1^{MKO} mice. We documented the infiltration of eosinophils and mast cells into the skin and higher levels of transcripts coding for Il-4, Il-5, Il-10, and Il-13 (the protein levels of cytokines Il-4 and Il-5 were also elevated). The presence of these transcripts in the skin is indicative of type 2 helper T-cell (Th2)-dominated immune responses [36,37]. Additional evidence of an allergen-specific elevation of Th2-cell generation was the levels of transcripts coding for chemokines typical of granulocytes, namely, Ccl2, -5, -7 and -11, in the skin of young Mcpip1^{MKO} mice, with greater intensity in older mice. Moreover, in the skin of transgenic mice, we observed the infiltration of M2-type macrophages (CD206 positive), which promote Th2-type immunity [38]. Suzuki and collaborators recently showed that large numbers of M2 macrophages accumulated in the sites of hapten-induced contact hypersensitivity (CHS), an animal model of allergic contact dermatitis [39]. Dysregulation of adaptive immunity in Mcpip1^{MKO} mice tending toward a Th2 cell-mediated immune response was also demonstrated by more intense spontaneous and chemically-induced skin contact allergy. In DTH reactions, T cells are first recruited to tissues and then activated by antigen-presenting cells to produce cytokines that mediate local inflammation [40]. Here, Mcpip1^{MKO} mice showed an intensified DTH response at two developmental stages: 12 and 24 weeks of age. This was demonstrated by an increase in ear swelling and significantly elevated levels of transcripts encoding cytokines and chemokines, such as Cxcl1, Cxcl2, Ccl5, Ccl11, Il-4, Il-5, and Il-6, which are typical of contact hypersensitivity inflammation [40,41]. This observation is another consequence presumably related to Th2 cell hyperactivation in the skin of Mcpip1^{MKO} mice, similar to the development of allergic skin conditions such as atopic dermatitis, which is generally a Th2-polarized disease [42].

It should be emphasized that the etiology of skin lesions in Mcpip1^{MKO} mice is more complex. More detailed analyses have also shown a Th1- (T helper type 1)-type immune response in the skin of Mcpip1^{MKO} mice; however, the Th2-dependent response was more pronounced. The Th1 response was mainly characterized by increased expression of *Ifng* mRNA, while the increase in the levels of the other Th1-dependent proinflammatory cytokines was significant in lesions but not in healthy skin of Mcpip1^{MKO} mice. The observed high expression of *Ifng* as well as signal transducers and activators of transcription (Stats) was confirmed by NGS analysis of the skin of Mcpip1^{MKO} mice (data not shown). Upregulation of Stat1 may be one of the drivers of high levels of *Ifng* mRNA in Mcpip1^{MKO} mice. Interferon-gamma (IFNg) was considered for many years to be a proinflammatory factor; however, there is some evidence showing its potent anti-inflammatory effect [43,44]. Many molecular mechanisms have been proposed to explain this phenomenon, including the role of IFNg in the regulation of T cell subsets. It was shown that the variable IL-4 and IL-5 phenotypes of Th2 cells are dependent on IFNg [45]. Clarification of which cells are responsible for the elevated level of this cytokine and its role in the skin of Mcpip1^{MKO} mice is currently under investigation.

The complexity of inflammatory changes in the skin of Mcpip1^{MKO} mice was also demonstrated when we applied imiquimod, as we showed only moderate psoriasis-like skin inflammation at a morphological level. Altogether, our data indicate that the most significant pathological change in the skin is allergic inflammation. Moreover, allergic inflammation is not limited to the skin but also manifests systemically. In the sera of Mcpip1^{MKO} mice, we observed significantly higher levels of IgE and an increased influx of eosinophils. Additional evidence of systemic allergic inflammation included significantly elevated levels of

transcripts coding for Gata3, Il-4, Il-5 and Il-13 in the lungs of Mcpip1^{MKO} mice (Suppl. Fig. 3). Furthermore, previously published results by our team showed that the levels of cytokines and chemokines, particularly Il-5, Il-10, Il-13, Ccl7 and Ccl11, were upregulated in the plasma of 24-week-old Mcpip1^{MKO} mice compared to control mice [46]. These animals were additionally characterized by reduced body mass, dyslipidemia (low cholesterol and HDL levels with a concomitant increase in LDL) and hypoglycemia. Metabolic changes in Mcpip1^{MKO} mice were not attributed to lower food consumption but were rather secondary to the inflammatory syndrome present in these animals [46]. The initiation of the Th2-type response occurs at tissue sites, including the gut, where microorganisms, their products or damage-associated molecular patterns are sensed by immune cells such as macrophages. The enhanced translocation of intestinal microorganisms outside the lumen leads to the response of tissue-distributed myeloid cells, which in turn secrete a range of cytokines that further promote Th2 cell differentiation. Among them is Il-4 [47,48], whose transcript level is elevated in the colons of Mcpip1^{MKO} mice. Moreover, we noted its increase in macrophages isolated from Mcpip1^{MKO} mice in response to intestinal bacteria and their PAMPs (LPS, CpG) compared to native cells. Elevated levels of *Il-4* were associated with increased expression of transcripts coding for C/ebpδ and β transcription factors, the levels of which were higher, especially in 24-week-old Mcpip1^{MKO} mice. C/EBPβ is implicated in cell differentiation and in the regulation of genes involved in immune and inflammatory responses and the induction of M2 macrophage-specific gene expression, including IL-4 [49,50]. Our previous studies have shown that knockdown of MCPIP1 results in the upregulation of C/EBPβ [51]; thus, the same mechanism could be responsible in Mcpip1^{MKO} mice. As C/EBPδ was also identified in the promoter sequence of IL-4, its role in the observed upregulation of IL-4 is highly possible [24]. Consequently, upregulation of C/ebpβ and C/ebpδ followed by the release of Il-4 preceded by intestinal dysbiosis in animals without phagocytic Mcpip1 promotes systemic allergic inflammation and consequently leads to skin allergy.

In conclusion, myeloid Mcpip1 deficiency causes intestinal dysbiosis, bacterial dissemination to peripheral organs and skin allergic inflammation. We propose that MCPIP1 in myeloid cells is a novel player that controls the gut-skin axis.

CRediT authorship contribution statement

Weronika Szukala: Data curation, Formal analysis, Funding acquisition, Investigation, Methodology, Visualization, Writing – original draft. **Magdalena Pilarczyk-Zurek:** Data curation, Formal analysis, Funding acquisition, Investigation, Methodology, Visualization, Writing – original draft. **Justyna Folkert:** Data curation, Formal analysis, Investigation. **Jerzy Kotlinowski:** Investigation, Methodology. **Joanna Koziel:** Conceptualization, Project administration, Resources, Supervision, Validation, Writing – original draft. **Jolanta Jura:** Conceptualization, Project administration, Resources, Supervision, Validation, Writing – original draft.

Declaration of competing interest

The authors declare the following financial interests/personal relationships which may be considered as potential competing interests: Jolanta Jura reports was provided by Jagiellonian Universityin Krakow, Faculty of Biochemistry, Biophysics and Biotechnology. Jolanta Jura reports a relationship with Jagiellonian University in Kraków Faculty of Biochemistry Biophysics and Biotechnology that includes:.

Data availability

Data will be made available on request.

Acknowledgments

We are grateful to the staff of the animal facility of the Faculty of Biochemistry, Biophysics and Biotechnology for help with animals breeding. This study was supported by National Science Centre grant number 2020/37/N/NZ5/00575 (to WS) and DEC-2020/04/X/NZ5/00546 (to MPZ). Open access publication of this article was funded by the Priority Research Area BioS under the program “Excellence Initiative – Research University” at Jagiellonian University in Krakow.

Appendix A. Supplementary data

Supplementary data to this article can be found online at https://doi.org/10.1016/j.bbadis.2023.166764.

References

[1] R. Kantor, J.I. Silverberg, Environmental risk factors and their role in the management of atopic dermatitis, Expert. Rev. Clin. Immunol. 13 (1) (2017) 15–26.
[2] M. Pasparakis, I. Haase, F.O. Nestle, Mechanisms regulating skin immunity and inflammation, Nat. Rev. Immunol. 14 (5) (2014) 289–301.
[3] J.A. Segre, Epidermal barrier formation and recovery in skin disorders, J. Clin. Invest. 116 (5) (2006) 1150–1158.
[4] C.A. O'Neill, G. Monteleone, J.T. McLaughlin, R. Paus, The gut-skin axis in health and disease: a paradigm with therapeutic implications, Bioessays. 38 (11) (2016) 1167–1176.
[5] C. Caffarelli, G. Cavagni, I. Menzies, P. Bertolini, D. Atherton, Elimination diet and intestinal permeability in atopic eczema: a preliminary study, Clin. Exp. Allergy 23 (1) (1993) 28–31.
[6] M. Candela, E. Biagi, S. Maccaferri, S. Turroni, P. Brigidi, Intestinal microbiota is a plastic factor responding to environmental changes, Trends Microbiol. 20 (8) (2012) 385–391.
[7] J. Penders, E.E. Stobberingh, Brandt Pvd, C. Thijs, The role of the intestinal microbiota in the development of atopic disorders, Allergy. 62 (11) (2007) 1223–1236.
[8] L.J. Pike, E.A. Kuenzel, J.E. Casnellie, E.G. Krebs, A comparison of the insulin-and epidermal growth factor-stimulated protein kinases from human placenta, J. Biol. Chem. 259 (15) (1984) 9913–9921.
[9] L. Monin, J.E. Gudjonsson, E.E. Childs, N. Amatya, X. Xing, A.H. Verma, et al., MCPIP1/regnase-1 restricts IL-17A–and IL-17C–dependent skin inflammation, J. Immunol. 198 (2) (2017) 767–775.
[10] E. Ruiz-Romeu, M. Ferran, A. Giménez-Arnau, B. Bugara, B. Lipert, J. Jura, et al., MCPIP1 RNase is aberrantly distributed in psoriatic epidermis and rapidly induced by IL-17A, J. Investig. Dermatol. 136 (8) (2016) 1599–1607.
[11] M. Takaishi, T. Satoh, S. Akira, S. Sano, Regnase-1, an immunomodulator, limits the IL-36/IL-36R autostimulatory loop in keratinocytes to suppress skin inflammation, J. Invest. Dermatol. 138 (6) (2018) 1439–1442.
[12] K. Matsushita, O. Takeuchi, D.M. Standley, Y. Kumagai, T. Kawagoe, T. Miyake, et al., Zc3h12a is an RNase essential for controlling immune responses by regulating mRNA decay, Nature. 458 (7242) (2009) 1185–1190.
[13] D. Mizgalska, P. Węgrzyn, K. Murzyn, A. Kasza, A. Koj, J. Jura, et al., Interleukin-1-inducible MCPIP protein has structural and functional properties of RNase and participates in degradation of IL-1β mRNA, FEBS J. 276 (24) (2009) 7386–7399.
[14] P. Konieczny, A. Lichawska-Cieslar, P. Kwiecinska, J. Cichy, R. Pietrzycka, W. Szukala, et al., Keratinocyte-specific ablation of Mcpip1 impairs skin integrity and promotes local and systemic inflammation, J. Mol. Med. 97 (12) (2019) 1669–1684.
[15] Y. Li, X. Huang, S. Huang, H. He, T. Lei, F. Saaoud, et al., Central role of myeloid MCPIP1 in protecting against LPS-induced inflammation and lung injury, Signal Transduct. Target. Ther. 2 (1) (2017) 1–15.
[16] E. Dobosz, G. Lorenz, A. Ribeiro, V. Würf, M. Wadowska, J. Kotlinowski, et al., Murine myeloid cell MCPIP1 suppresses autoimmunity by regulating B-cell expansion and differentiation, Dis. Model. Mech. 14 (3) (2021), dmm047589.
[17] L. Röse, C. Schneider, C. Stock, T.M. Zollner, W.D. Döcke, Extended DNFB-induced contact hypersensitivity models display characteristics of chronic inflammatory dermatoses, Exp. Dermatol. 21 (1) (2012) 25–31.
[18] L. Van Der Fits, S. Mourits, J.S. Voerman, M. Kant, L. Boon, J.D. Laman, et al., Imiquimod-induced psoriasis-like skin inflammation in mice is mediated via the IL-23/IL-17 axis, J. Immunol. 182 (9) (2009) 5836–5845.
[19] M.S. Lindner, B.Y. Renard, Metagenomic abundance estimation and diagnostic testing on species level, Nucleic Acids Res. 41(1):e10-e (2013).
[20] M.B. Pereira, M. Wallroth, V. Jonsson, E. Kristiansson, Comparison of normalization methods for the analysis of metagenomic gene abundance data, BMC Genomics 19 (2018) 1–17.
[21] M. Wadowska, E. Dobosz, A. Golda, D. Bryzek, M. Lech, M. Fu, et al., MCP-induced protein 1 participates in macrophage-dependent endotoxin tolerance, J. Immunol. 209 (7) (2022) 1348–1358.
[22] C.E. West, M. Jenmalm, S. Prescott, The gut microbiota and its role in the development of allergic disease: a wider perspective, Clin. Exp. Allergy 45 (1) (2015) 43–53.

[23] A.C. McPherson, S.P. Pandey, M.J. Bender, M. Meisel, Systemic immunoregulatory consequences of gut commensal translocation, Trends Immunol. 42 (2) (2021) 137–150.
[24] M. Li-Weber, O. Laur, I.V. Davydovv, C. Hu, P. Salgame, P.H. Krammer, What controls tissue-specific expression of the IL-4 gene? Immunobiology. 198 (1–3) (1997) 170–178.
[25] W.E. Paul, J. Zhu, How are TH2-type immune responses initiated and amplified? Nat. Rev. Immunol. 10 (4) (2010) 225–235.
[26] T.D. Lawley, A.W. Walker, Intestinal colonization resistance, Immunology. 138 (1) (2013) 1–11.
[27] P. Das, P. Babaei, J. Nielsen, Metagenomic analysis of microbe-mediated vitamin metabolism in the human gut microbiome, BMC Genomics 20 (2019) 1–11.
[28] N. Kamada, S.-U. Seo, G.Y. Chen, G. Núñez, Role of the gut microbiota in immunity and inflammatory disease, Nat. Rev. Immunol. 13 (5) (2013) 321–335.
[29] R.E. Ley, M. Hamady, C. Lozupone, P.J. Turnbaugh, R.R. Ramey, J.S. Bircher, et al., Evolution of mammals and their gut microbes, Science 320 (5883) (2008) 1647–1651.
[30] M. Levy, A.A. Kolodziejczyk, C.A. Thaiss, E. Elinav, Dysbiosis and the immune system, Nat. Rev. Immunol. 17 (4) (2017) 219–232.
[31] Y. Belkaid, T.W. Hand, Role of the microbiota in immunity and inflammation, Cell. 157 (1) (2014) 121–141.
[32] M.E. Johansson, M. Phillipson, J. Petersson, A. Velcich, L. Holm, G.C. Hansson, The inner of the two Muc2 mucin-dependent mucus layers in colon is devoid of bacteria, Proc. Natl. Acad. Sci. 105 (39) (2008) 15064–15069.
[33] H. Bisgaard, N. Li, K. Bonnelykke, B.L.K. Chawes, T. Skov, G. Paludan-Müller, et al., Reduced diversity of the intestinal microbiota during infancy is associated with increased risk of allergic disease at school age, J. Allergy Clin. Immunol. 128 (3) (2011) 646–652 (e5).
[34] K. Mah, B. Björkstén, B. Lee, H. Van Bever, L. Shek, T. Tan, et al., Distinct pattern of commensal gut microbiota in toddlers with eczema, Int. Arch. Allergy Immunol. 140 (2) (2006) 157–163.
[35] L. Nylund, M. Nermes, E. Isolauri, S. Salminen, W. De Vos, R. Satokari, Severity of atopic disease inversely correlates with intestinal microbiota diversity and butyrate-producing bacteria, Allergy. 70 (2) (2015) 241–244.
[36] F. Davoine, P. Lacy, Eosinophil cytokines, chemokines, and growth factors: emerging roles in immunity, Front. Immunol. 5 (2014) 570.
[37] S.J. Galli, M. Maurer, C.S. Lantz, Mast cells as sentinels of innate immunity, Curr. Opin. Immunol. 11 (1) (1999) 53–59.
[38] T.A. Wynn, K.M. Vannella, Macrophages in tissue repair, regeneration, and fibrosis, Immunity. 44 (3) (2016) 450–462.
[39] K. Suzuki, K. Meguro, D. Nakagomi, H. Nakajima, Roles of alternatively activated M2 macrophages in allergic contact dermatitis, Allergol. Int. 66 (3) (2017) 392–397.
[40] R.S. Kalish, P.W. Askenase, Molecular mechanisms of CD8+ T cell–mediated delayed hypersensitivity: implications for allergies, asthma, and autoimmunity, J. Allergy Clin. Immunol. 103 (2) (1999) 192–199.
[41] K. Kobayashi, K. Kaneda, T. Kasama, Immunopathogenesis of delayed-type hypersensitivity, Microsc. Res. Tech. 53 (4) (2001) 241–245.
[42] Y. Tokura, P. Phadungsaksawasdi, T. Ito, Atopic dermatitis as Th2 disease revisited, J. Cutan. Immunol. Allergy 1 (5) (2018) 158–164.
[43] H. Kelchtermans, A. Billiau, P. Matthys, How interferon-γ keeps autoimmune diseases in check, Trends Immunol. 29 (10) (2008) 479–486.
[44] H. Kelchtermans, B. De Klerck, T. Mitera, M. Van Balen, D. Bullens, A. Billiau, et al., Defective CD4+ CD25+ regulatory T cell functioning in collagen-induced arthritis: an important factor in pathogenesis, counter-regulated by endogenous IFN-γ, Arthritis Res. Ther. 7 (2005) 1–14.
[45] A. Wensky, Garibaldi Marcondes, MCl, Lafaille JJ., The role of IFN-γ in the production of Th2 subpopulations: implications for variable Th2-mediated pathologies in autoimmunity, J. Immunol. 167 (6) (2001) 3074–3081.
[46] N. Pydyn, D. Żurawek, J. Kozieł, E. Kus, K. Wojnar-Lason, A. Jasztal, et al., Role of Mcpip1 in obesity-induced hepatic steatosis as determined by myeloid and liver-specific conditional knockouts, FEBS J. 288 (22) (2021) 6563–6580.
[47] G. Le Gros, S.Z. Ben-Sasson, R. Seder, F.D. Finkelman, W. Paul, Generation of interleukin 4 (IL-4)-producing cells in vivo and in vitro: IL-2 and IL-4 are required for in vitro generation of IL-4-producing cells, J. Exp. Med. 172 (3) (1990) 921–929.
[48] S.L. Swain, A.D. Weinberg, M. English, G. Huston, IL-4 directs the development of Th2-like helper effectors, J. Immunol. 145 (11) (1990) 3796–3806.
[49] D. Ruffell, F. Mourkioti, A. Gambardella, P. Kirstetter, R.G. Lopez, N. Rosenthal, et al., A CREB-C/EBPβ cascade induces M2 macrophage-specific gene expression and promotes muscle injury repair, Proc. Natl. Acad. Sci. 106 (41) (2009) 17475–17480.
[50] F. Berberich-Siebelt, S. Klein-Hessling, N. Hepping, B. Santner-Nanan, D. Lindemann, A. Schimpl, et al., C/EBPβ enhances IL-4 but impairs IL-2 and IFN-γ induction in T cells, Eur. J. Immunol. 30 (9) (2000) 2576–2585.
[51] B. Lipert, M. Wilamowski, A. Gorecki, J. Jura, MCPIP1, alias Regnase-1 binds and cleaves mRNA of C/EBPβ, PLoS One 12 (3) (2017), e0174381.